Natural and designed proteins inspired by extremotolerant organisms can form condensates and attenuate apoptosis in human cells

Mike T. Veling[1,2,7], Dan T. Nguyen[1,2,7], Nicole N. Thadani[1], Michela E. Oster[1,2], Nathan J. Rollins[1,2], Kelly P. Brock[1], Neville P. Bethel[3,4], David Baker[3,4,5], Jeffrey C. Way[1,2], Debora S. Marks[1,6], Roger L. Chang[1,2,8], Pamela A. Silver[1,2,8]

Affiliations

1. Department of Systems Biology, Harvard Medical School, Boston, MA, 02115, USA;
2. Wyss Institute for Biologically Inspired Engineering, Boston, MA, 02115, USA;
3. Institute for Protein Design, University of Washington, Seattle, WA, 98195, USA;
4. Department of Biochemistry, University of Washington, Seattle, WA, 98195, USA;
5. Howard Hughes Medical Institute, University of Washington, Seattle, WA, 98195, USA;
6. Broad Institute of Harvard and MIT, Cambridge, MA, 02142, USA;
7. Co-first authors
8. Co-corresponding authors

Key words

Stress tolerance, Phase separation, Intrinsically disordered proteins, Apoptosis

ABSTRACT

Many organisms can survive extreme conditions and successfully recover to normal life. This extremotolerant behavior has been attributed in part to repetitive, amphipathic, and intrinsically disordered proteins that are upregulated in the protected state. Here, we assemble a library of approximately 300 naturally-occurring and designed extremotolerance-associated proteins to assess their ability to protect human cells from chemically-induced apoptosis. We show that proteins from tardigrades, nematodes, and the Chinese giant salamander are apoptosis protective. Notably, we identify a region of the human ApoE protein with similarity to extremotolerance-associated proteins that also protects against apoptosis. This region mirrors the phase separation behavior seen with such proteins, like the tardigrade protein CAHS2. Moreover, we identify a synthetic protein, DHR81, that shares this combination of elevated phase separation propensity and apoptosis protection. Finally, we demonstrate that driving protective proteins into the condensate state increases apoptosis protection, and highlight the ability for DHR81 condensates to sequester caspase-7. Taken together, this work draws a link between extremotolerance-associated proteins, condensate formation, and human cellular protection.

INTRODUCTION

When exposed to extreme environmental stress, extremotolerance-associated (*ExTol*) organisms enter a state of reduced cellular metabolic activity that promotes survival in harsh conditions. This state has been shown to protect these organisms from high salinity, desiccation, and even the vacuum of outer space (Jonsson et al., 2008). To acclimate to

47 these conditions, *ExTol* organisms significantly upregulate the production of protective
48 metabolites, like trehalose (Neuman, 2006), as well as tolerance-conferring proteins
49 (Boothby et al., 2017), many of which are intrinsically disordered proteins (*IDPs*) with
50 repetitive sequence and predicted amphipathic helices.
51
52 While the mechanism of protection is unknown, one model suggests these proteins
53 mediate formation of a gel- or glass-like material state within an entire cell to protect it
54 from damage (Boothby et al., 2017; Hengherr et al., 2008). The model posits that such
55 proteins promiscuously interact with membranes and proteins, increasing intracellular
56 viscosity and protecting vulnerable structures (Hand et al., 2011) (Figure 1A Top). Such
57 interactions would also work to prevent stress-induced protein unfolding and protein
58 aggregation (Chakrabortee et al., 2010). An alternative model suggests that these
59 proteins form intracellular phase-separated membraneless compartments with distinct
60 physical parameters (referred to here as *condensates*) that partition key stress-sensitive
61 cellular components (Belott et al., 2020) (Figure 1A Bottom). Within these dense protein
62 structures, essential components are sequestered and protected from damage. The
63 models are not mutually exclusive; for example, in the case of desiccation tolerance,
64 continued dehydration could lead phase-separated compartments to fuse, comprise
65 much (if not all) of the cell, and promote a glassy material state.
66
67 The resurgence of interest in biological phase separation, extensively reviewed in
68 (Boeynaems et al., 2018; Choi et al., 2020; Hyman et al., 2014; Shin and Brangwynne,
69 2017), has shown that human cells can employ similar strategies to survive stressful

70 conditions. While the reversible formation of stress granules in healthy cells is the
71 archetype of stress tolerance, recent studies have revealed phase separation as a key
72 adaptation that cancer cells use to avoid apoptosis and cell death (Jiang et al., 2020).
73 Phase-separated condensates have been implicated in sequestering key tumor
74 repressors (Jiang et al., 2020), enhancing or repressing gene expression in response to
75 stress (Boija et al., 2018), and concentrating and protecting key metabolites like
76 nucleotides (Hubstenberger et al., 2017). These processes parallel the mechanisms that
77 ExTol proteins are thought to use to protect complex biological systems, suggesting there
78 could be some functional overlap. That is, sequence features and properties within ExTol
79 proteins could be implicated in mammalian stress tolerance pathways, including
80 apoptosis resistance.
81
82 A key sequence feature of some ExTol proteins is the presence of amphipathic helices
83 (Tolleter et al., 2007). While disordered in most contexts, ExTol proteins can transiently
84 form amphipathic helices in certain molecular environments, notably when interacting with
85 and stabilizing membranes (Hand et al., 2011). The helices often exhibit a hydrophobic
86 face, which interacts with core lipids within the membrane, flanked by positively charged
87 residues that might interact with the negatively charged lipid head groups (Figure 1B).
88 This amphipathic moment often repeats across the length of the protein (Figure 1C). This
89 feature is a hallmark of the late embryonic abundant (LEA) class of ExTol proteins (Hand
90 et al., 2011). Human membrane interacting proteins, like alpha-synuclein, also exhibit a
91 similar repeat motif (Bussell and Eliezer, 2003). Such parallels in sequence features

92 suggest that orthogonal expression of ExTol proteins may confer their protective
93 properties to other biological systems, like human cells.
94
95 Indeed, previous reports have shown that some of these ExTol proteins provide similar
96 protective properties when expressed heterologously. Expressing tardigrade-specific
97 IDPs (TDPs) in bacteria provides protection against desiccation (Boothby et al., 2017).
98 Anhydrin, an IDP upregulated by *Aphelenchus avenae* during dehydration, expressed in
99 a human cell line limited PABPN1-A17 aggregation, a hallmark of oculopharyngeal
100 muscular dystrophy (Chakrabortee et al., 2010). Similar reports demonstrated protection
101 of human cells provided by expression of LEA proteins originating from the African midge
102 (Li et al., 2012) and by TDPs from tardigrades (Tanaka et al., 2015). These findings
103 reinforce the promise of transferring protective phenotypes from their native contexts to
104 human cells.
105
106 Taken together, these data indicate a potential avenue for using this class of proteins to
107 protect biological systems in a controlled manner. To test this hypothesis, we generated
108 approximately 300 sequences inspired by ExTol proteins and examined their ability to
109 protect against apoptotic cell death. Our results show that human proteins containing
110 sequence hallmarks of ExTol proteins as well as *de-novo* designed condensate forming
111 proteins can protect human cells from chemically-induced apoptosis. We also
112 demonstrate that condensate induction using synthetic modifications can strengthen
113 apoptotic protection. Finally, we show that key components of the apoptotic pathway can

114 localize to inducible condensates, suggesting enzyme sequestration could be a
115 mechanism of action.
116
117 **RESULTS**
118 **Assembling a library of stress tolerance proteins**
119 Based on the hallmark sequence features of ExTol proteins, we searched the published
120 literature to identify proteins that not only contain these features but also exhibit some
121 evidence for protection of biological structures. The library was generated based on over
122 one hundred naturally-occurring proteins based on five lines of evidence for stress
123 tolerance association, including: change in expression during extremotolerance,
124 knockdown or overexpression changing the tolerant state, *in vitro* protection, orthogonal
125 expression transferring tolerance, and sequence similarity to other proteins with these
126 features (Figure 1D and Supplemental table 1).
127
128 A PFAM domain analysis of the identified proteins reveals almost half of the identified
129 targets have two key domains: Late Embryonic Abundant (LEA) and Apolipoprotein E
130 (ApoE) domains (Figure 1E, Supplemental table 1). LEA proteins are well known to be
131 upregulated during the last stages of plant seed maturation (Mertens et al., 2018). This
132 domain is thought to protect the seed embryo during transport to its new destination.
133 There is also evidence that this domain has been co-opted by bacteria as protection from
134 desiccation and radiation (Makarova et al., 2001). ApoE proteins interact with lipid
135 particles to allow for lipid reuptake into cells. Additionally, mutations within human ApoE
136 have been identified as strong genetic predictors of Alzheimer's disease in human

137 populations (Yamazaki et al., 2019). Based on their lipid interaction properties and
138 potential role in neuronal homeostasis, as well as its prevalence in the PFAM domain
139 analysis, we decided to include human ApoE and its various mutations in our study as an
140 ExTol protein.
141
142 **Designing novel extremotolerance-associated proteins**
143 To test hypotheses about sequence features and their relationship to phase separation
144 and apoptosis, we designed novel proteins based on the set of ExTol proteins. These
145 new designs take 3 approaches (Figure 2): truncation of proteins to focus on repetitive,
146 intrinsically disordered, and amphipathic regions; isolation of individual helices with
147 desired sequence features; and *de novo* design of alpha helix-containing proteins that
148 self-assemble into higher order structures. Through these designs, we sought to identify
149 the minimal elements required for protection and phase separation.
150
151 First, we identified regions within natural proteins that contain intrinsic disorder (Erdos
152 and Dosztanyi, 2020), repetitive sequences (Biegert and Soding, 2008), and amphipathic
153 helices (Gimenez-Andres et al., 2018; Segrest et al., 1992). Figure 2A illustrates the use
154 of HHRepID on the sequence of full length human ApoE. Based on this analysis, we
155 identified the repeating domain within ApoE for further testing. Other ExTol proteins were
156 similarly modified and examined.
157
158 We also included short peptides based on the consensus sequence of repetitive regions
159 that have previously been shown to be protective (Furuki et al., 2019). To test if any of

160 the sequence features we identified are important for apoptosis protection, we altered
161 these features within these short peptides. For example, we altered the amphipathic
162 character of these helices (Figure 2B) to determine if apoptosis protection was changed.
163
164 To examine whether generic condensate formation is sufficient to confer apoptosis
165 protection, we also examined completely synthetic alpha helix-containing proteins that
166 were designed to form repetitive structure with sequences orthogonal to naturally-
167 occurring proteins (Brunette et al., 2015). These designed helical repeat (DHR) proteins
168 interact along the axis of the helix, forming long spiraling fibrils, but may also potentially
169 self-interact along the face of the protein based on a pattern of positive and negative
170 charges (Figure 2C). This ability to oligomerize and form multivalent complexes, which
171 may then interact via weak non-covalent interactions, is an established determinant of
172 condensate formation (Choi et al., 2020).
173
174 Together, our library consists of 104 naturally-occurring proteins, 166 truncations or
175 isolations of helical regions, and 19 *de novo* designs (Figure 2D). Taken altogether, these
176 proteins interrogate several hypotheses about how disordered proteins may protect
177 human cells against apoptosis.
178
179 **Apoptosis assay identifies extremotolerance-associated proteins in human cells**
180 To model stress in a mammalian cell system, we induced cellular apoptosis by treatment
181 with the chemotherapeutic camptothecin (CPT), a DNA topoisomerase inhibitor well
182 known to trigger apoptosis (Li et al., 2017; Wall et al., 1966). Under these conditions,

183 protection against apoptosis could be achieved through a number of avenues, including
184 protection against the DNA damage caused by CPT-induced topoisomerase inhibition (Li
185 et al., 2017), interruption of the signaling cascade, or even protection of the mitochondrial
186 membrane whose rupture ultimately triggers apoptosis (Bortner and Cidlowski, 2002).
187
188 To test our designs for protection against apoptosis, we used a human cell-based
189 apoptosis assay (Figure 3A). This assay uses HT-1080 fibrosarcoma cells from ATCC
190 (Rasheed et al., 1974). These cells are seeded in a 96-well plate and allowed to adhere
191 overnight. The next day, the cells are co-transfected with a plasmid containing the ExTol
192 candidate proteins of interest as well as a transfection marker. The following day, the
193 media is swapped to one containing 13.2 μM CPT. After addition of CPT, caspase-3 and
194 -7 activation is measured by microscopy every 45 minutes for 1 day using a fluorophore
195 quencher pair attached to either end of a peptide with the sequence “DEVD”. As caspase-
196 3 and -7 are activated, the DEVD peptide is cleaved, releasing the fluorophore from the
197 quencher. The unquenched fluorophore localizes to the nucleus where it can be
198 quantified by imaging on a single-cell level. The single-cell resolution allows for the
199 separation of transfected and non-transfected cells based on the transfection marker.
200 Only single cells with the transfection marker were subjected to further analysis; Figure
201 3B shows sample images highlighting the type of data being analyzed.
202
203 On every plate, an empty vector negative control is run as well as a positive control
204 containing the X-linked inhibitor of apoptosis (XIAP). This protein is known to bind to
205 caspase-3 and -7 to block their activity (Obexer and Ausserlechner, 2014) . Figure 3C

206 shows example data comparing median DEVD peptide signal intensity over time after
207 induction with CPT of four wells on the same plate transfected with XIAP and empty
208 vector. The results show a reduction in DEVD peptide signal intensity when the XIAP-
209 containing vector is transfected, demonstrating that the assay can identify modulators of
210 apoptosis.
211
212 To convert these time-resolved data to a measure of protection against apoptosis, the
213 maximum DEVD peptide signal intensity is calculated and normalized to a plate-matched
214 empty vector control (see methods for further details). The normalized apoptosis induction
215 intensity is shown in Figure 3D left. The data are slightly skewed towards apoptosis-
216 protection, which supports our hypothesis that the targeted proteins can protect against
217 apoptosis.
218
219 To highlight the top-performing designs, the top 10% of the targets are shown in Figure
220 3D right. As expected, the XIAP positive control showed the strongest anti-apoptotic
221 effect. The two top-performing hits were ApoE designs. Human alpha-synuclein is the 5th
222 hit, which is expected as it is known to be both intrinsically disordered, and anti-apoptotic
223 (Li and Lee, 2005). Additionally, several ApoE designs and short LEA helices are top hits.
224 The data used to generate these figures is included in supplemental table 2.
225
226 **Known extremotolerance-associated proteins affect apoptosis**
227 Among the top hits in apoptosis reduction are an IGKV protein highly expressed in mucus
228 of the Chinese giant salamander *Andrias davidianus* (Geng et al., 2019) that is used as

229 a medical glue in traditional Chinese medicine, an LEA protein from the nematode
230 *Aphelenchus avenae* previously shown to have the ability to reduce a form of protein
231 aggregation associated with oculopharyngeal muscular dystrophy in human cells
232 (Chakrabortee et al., 2010), and a mitochondrial LEA protein from the brine shrimp
233 *Artemia franciscana* shown to protect human cells during desiccation (Li et al., 2012)
234 (Figure 3D). The prominence of these ExTol proteins suggests the assay can help identify
235 other proteins that can protect cells from more general stresses beyond CPT-induced
236 apoptosis.
237
238 **Short repetitive peptides and *de novo* designs modulate apoptosis**
239 LEA repeat-containing peptides are among the top-performing hits in the screen. While
240 the original short LEA designs from Furuki et al. 2019 (Furuki et al., 2019) had a minor
241 effect reducing apoptosis, several of the designs tested here performed better
242 (Supplemental Figure 3A). As 22 amino acids is small and could lead to peptide stability
243 issues, longer 50-amino acid designs inspired by the same LEA proteins Furuki et al.
244 utilized were also developed (Supplemental Figure 3B). Some of these designs were also
245 able to reduce apoptosis, including the PvLEA4 with extended repeats (notably PvLEA4
246 repeats extended #2), which fell into the top hits of the entire library (Figure 3D and
247 Supplemental Figure 3B). These results suggest that optimization of synthetic designs
248 yields proteins with stronger function than naturally-occurring proteins.
249
250 While these proteins were designed to interrogate the relationship between sequence
251 and apoptosis protection in short peptides, little relationship was found with respect to the

252 sequence features we analyzed (Supplemental Figure 3C). Several designs were made
253 that would alter the hydrophobic moments of putative helices these peptides are predicted
254 to form. To examine if this sequence property relates to the stress-tolerance function of
255 these proteins, we attempted to correlate this property with assay performance. However,
256 no significant correlation was found, suggesting (at least in these cases) that degree of
257 amphipathicity on its own is not the key determinant of stress-tolerance function of these
258 proteins.
259
260 **The repeat region of ApoE comprises its minimal anti-apoptotic unit**
261 The top two hits in the assay were ApoE4 (47-300) and ApoE2 (47-300). These truncated
262 forms of ApoE maintain the repeat domains shown in Figure 4A, while removing the signal
263 peptide and terminal regions. This suggests that the repeat region of ApoE accounts for
264 its core anti-apoptotic functionality. Interestingly, the full length ApoE2 and E4 do not
265 show up as top hits, suggesting that these truncated forms improve on the apoptosis
266 protection provided by the full-length variants (Figure 4B).
267
268 Based on the location of the signal peptide, it is expected that ApoE4 should localize to
269 the secretory pathway whereas the truncated form may be cytoplasmic. To test this
270 hypothesis, cells were subjected to Western blot and immunofluorescence analysis using
271 commercially available antibodies (Abcam ab24139; Figure 4C and Supplemental Figure
272 4A). The Western blot results show that both the full-length and truncated forms of ApoE4
273 are expressed at the expected size (Supplemental Figure 4A). The immunofluorescence
274 shows co-localization between the ApoE4 full length protein and the endoplasmic

275 reticulum (marked by Thermo's PDI antibody MA3-019, Figure 4C). However, the
276 truncated form did not show the same co-localization, suggesting as expected that it may
277 not enter the secretory pathway as the full-length version does.
278
279 Strikingly, the truncated version appeared to form more pronounced puncta throughout
280 the cytoplasm of the cell, suggesting the formation of potentially phase-separated
281 condensates. In screening through the point mutants of ApoE also tested here, we found
282 a similar condensate phenotype with the full length ApoE3 D125I mutation (Supplemental
283 Figure 4B). Together, these data suggest that ApoE may be able to support condensate
284 formation and confer apoptosis protection in part via the protective compartment
285 mechanism (Figure 1A bottom).
286
287 **CAHS2 and ApoE form condensates upon induced multivalency**
288 Established condensate engineering tools (Bracha et al., 2019) were used to test for
289 latent phase separation propensity within the top performing proteins. We used both light-
290 and chemically-inducible systems of multivalency. In the light system, a ferritin core
291 (comprised of self-assembled monomers, FTH1 domain-eGFP-iLID) becomes decorated
292 with SspB-modified proteins upon exposure to blue light (Bracha et al., 2018) (Figure 4D
293 top). In the chemical system, multivalency (i.e. multiple arms of the ExTol protein of
294 interest) is induced using a dimerization agent (Stanton et al., 2018) that brings together
295 FKBP-modified proteins (Bracha et al., 2019) (Figure 4D bottom). These inducible
296 methods increase the valency of a system, and thus work to favor phase separation. In

297 this way, they can help reveal any latent ability to form condensates that is not
298 immediately observable without modification.
299
300 Indeed, condensates were observed in both inducible systems using ExTol proteins.
301 CAHS2, a protein from the tardigrade *P. richtersi*, exhibited the most dramatic phenotype,
302 which is consistent with recent work describing the gel forming capabilities of CAHS
303 proteins (Yagi-Utsumi et al., 2021) (Figure 4E&F). ApoE variants were of particular
304 interest, based on the puncta observed in the top performing ApoE constructs. All
305 versions of ApoE tested formed puncta without activation, consistent with our previous
306 observation using untagged native ApoE (Figure 4C). Upon light- or chemical-activation,
307 there is a noticeable increase in condensates, exemplifying how phase separation can be
308 enhanced with increased multivalency (Figure 4E&F).
309
310 **Induction of condensates reduces apoptosis**
311 Induction of multivalency in ApoE containing constructs reduces apoptosis. We performed
312 the apoptosis assay using the top hits modified for chemically-induced multivalency,
313 namely fusion to two FKBP domains. The results show that the presence of the chemical
314 dimerizer did not affect apoptosis signal in cells transfected with the empty vector; in
315 contrast, the ApoE constructs exhibit reduced apoptosis with added dimerizer (Figure
316 4G). That is, artificially increasing ApoE condensates was apoptosis protective. These
317 data suggest that condensate formation plays a role in the anti-apoptotic effect of these
318 proteins.
319

320 **Synthetic DHR81 condensates reduce apoptosis and sequester caspase-7**

321 Induction of DHR81 based condensates protects against apoptosis. DHR81 is formed
322 from four helical hairpin repeat regions; the core of the protein is hydrophobic to ensure
323 consistent folding, while the outside of the protein is decorated with checkerboard positive
324 and negative charges (Figure 5A) (Brunette et al., 2015). This structure ensures the
325 protein is well folded, while also enabling the potential for higher order structure formation
326 via electrostatic interactions. Indeed, as with the ApoE variants, DHR81 supported
327 condensates in the chemically-inducible condensate system (Figure 5B) and exhibited a
328 stronger anti-apoptotic phenotype when multivalency is induced (Figure 5C and
329 Supplemental Figure 5A). There was little to no effect in cells containing an empty vector
330 or expressing the FKBP dimerization domains alone.

331

332 To further explore how condensates mediated by ExTol proteins may confer an anti-
333 apoptotic effect, we examined whether they sequester major components of apoptotic
334 signaling, namely caspase-3 and -7. The results showed that activated caspase-7
335 localized to DHR81 condensates but not CAHS2 or ApoE4 condensates (Figure 5D).
336 Caspase-3, however, does not localize to either DHR81, CAHS2, or ApoE4 condensates
337 (Supplemental Figure 5B). These results suggest sequestration of key apoptotic factors
338 could be a mechanism by which these condensates reduce apoptosis.

339

340 **Discussion**

341 To broadly evaluate the ability of ExTol proteins to protect orthogonal systems from
342 environmental stress, we studied over one hundred different ExTol proteins. We used

343 these as a basis to design approximately 300 variants, including truncations and fusion
344 proteins. These designs were evaluated on their ability to protect human HT-1080 cells
345 against CPT-induced apoptosis. The results showed that known ExTol proteins, ApoE
346 variants, and the synthetic DHR81 protein could modulate apoptosis levels when
347 transferred to human cells.
348
349 Protection against apoptosis is a key feature of many ExTol proteins. As apoptosis is a
350 common cellular response to stress, the ability to mitigate this response is important in
351 providing cell-autonomous protection in stressful environments. While the mechanism
352 resilient organisms use to survive is still not fully understood, it is becoming increasingly
353 clear that phase separation may play an important role.
354
355 ExTol proteins are proposed to form expansive higher order structures (e.g. gels or glassy
356 systems) that reduce the viscosity of the cytoplasm, especially in desiccated states
357 (Boothby et al., 2017). Other reports show that these proteins could mediate formation of
358 protective phase-separated compartments (i.e. condensates), sequestering damage-
359 inducing proteins and/or protecting important targets (Belott et al., 2020). Based on our
360 condensate data, it appears the latter may be at play for proteins like ApoE or DHR81.
361 Notably, in these proteins that already exhibit both anti-apoptotic effects as well as
362 elevated phase separation propensities, increasing the amount of condensates via an
363 engineered inducible system improved protection against apoptosis. This observation
364 suggests that condensates could be a key part of the protective mechanism.
365

366 Interestingly, we observed that activated caspase-7 partitions into DHR81 condensates,
367 suggesting caspase sequestration as a potential anti-apoptotic mechanism. Phase-
368 separated condensates and higher order assemblies are already implicated in mediating
369 apoptosis: stress granules inhibit apoptosis by suppressing MAPK pathways (Arimoto et
370 al., 2008); paraspeckles sequester pro-apoptotic tumor suppressors (Jiang et al., 2020);
371 the apoptosome relies on Apaf-1 multimerization, which has been reported to undergo
372 amyloid fibrillation in specific conditions (Rao et al., 2009); and stress-dependent phase
373 separation modulates proteasome formation, whose function affects apoptosis (Gupta et
374 al., 2018; Yasuda et al., 2020). It is interesting to note that we only observe clear caspase-
375 7 partitioning into DHR81 condensates, suggesting the possibility of a specific binding
376 interaction in this case. ApoE condensates may be sequestering other apoptotic factors
377 or using a different mechanism to reduce apoptosis.
378
379 It is also possible that these ExTol proteins achieve their anti-apoptotic effect by
380 implementing a more general physical mechanism, namely slowing the intracellular
381 mobility of biological effectors. There are various reports describing how the effective
382 viscosity within the cytoplasm can be increased in response to external stresses
383 (Dijksterhuis et al., 2007; Parry et al., 2014) or mediated by protein composition,
384 specifically intrinsically disordered proteins (Theillet et al., 2014). Notably, a pervasive
385 cell-spanning gel or network is not necessary to achieve such an effect; it is possible that
386 the presence of condensates, coupled with their ability to selectively partition
387 biomolecules (i.e. control what biomolecules can enter and diffuse through them), could
388 broadly slow biomolecular movement. That is, by forcing different proteins to either be

389 trapped in them or diffuse around them, condensates can decrease protein mobility and
390 perturb e.g. signaling pathways. Our results showing a lack of caspase-7 sequestration
391 by some of our protein condensates could thus support this more general mechanism of
392 condensates perturbing biology.
393
394 Condensates are becoming increasingly implicated in disease (Shin and Brangwynne,
395 2017), particularly when their structural metastability and reversibility is dysregulated (e.g.
396 through mutation). Notably, drugs that block the formation of amyloid fibrils and plaques,
397 which are products of phase separation dysregulation, are promising yet strongly debated
398 (Lalli et al., 2021) therapies for many neurological diseases. As such, our observations of
399 ApoE are particularly salient. We found that expression of a cytoplasmic form of ApoE is
400 protective against apoptosis. In particular, the truncated repeat region of ApoE is sufficient
401 and shows the strongest anti-apoptotic activity of all designs we tested. Others have
402 shown similar effects for exogenously added ApoE-containing liposomes protecting rat
403 neurons against apoptosis (Hayashi et al., 2009), though we show the effect through
404 overexpression of ApoE inside of human cells. When combined with our condensate
405 results and the clinical relevance of ApoE in Alzheimer's disease (Schellenberg et al.,
406 2000), these observations suggest the anti-apoptotic effect observed here warrants
407 further study, to further elucidate its role in Alzheimer's disease progression.
408
409 Altogether, our work expands upon the understanding of the relationship between
410 condensate formation and cell physiology, demonstrating how condensate accumulation

411 can be broadly beneficial in reducing apoptosis while also identifying diverse new protein
412 domains that confer protection.
413

414 **Author Contributions**

415 M.T.V. and D.T.N. designed and performed experiments, analyzed the data, and wrote
416 the paper. N.N.T. analyzed the data and wrote the paper. M.E.O provided technical
417 support. N.J.R., K.B.B., and N.P.B., designed constructs. D.B. and J.C.W. managed the
418 teams and provided key insight. D.S.M., R.L.C., and P.A.S., designed constructs,
419 managed teams, and wrote the paper.
420

421 **Acknowledgements**

422 Research was sponsored by the NSF, DARPA, the Wyss Institute for Biologically inspired
423 engineering, and the Army Research Office and was accomplished under Cooperative
424 Agreement Number W911NF-19-2-0017. M.T.V. was sponsored by the National Science
425 Foundation under Grant No. 2010370. D.T.N., N.N.T., M.E.O., N.J.R., K.P.B., J.C.W,
426 D.S.M., and P.A.S. were supported by the Harvard Medical School Department of
427 Systems Biology. J.C.W. was further supported by the Harvard Medical School
428 Laboratory of Systems Pharmacology. K.P.B. and D.S.M. were further supported by CZI
429 Neurodegenerative Challenge Ben Barres Early Career Award (CZI2018-191853). N.P.B
430 was further supported by the HHMI Hanna Gray fellowship (grant GT11817). We would
431 like to acknowledge Clarence Yapp for help with microscopy as well as the NCI U54-
432 CA225088 grant and a gift from the Ludwig Institute for Cancer Research to the
433 Laboratory for Systems Pharmacology. We would like to acknowledge the Nikon Imaging

434 Center at Harvard Medical Center for providing microscope support. The views and
435 conclusions contained in this document are those of the authors and should not be
436 interpreted as representing the official policies, either expressed or implied, of any funding
437 agency including the NSF, DARPA, the Army Research Office, or the U.S. Government.
438 The U.S. Government is authorized to reproduce and distribute reprints for Government
439 purposes notwithstanding any copyright notation herein.

440

441 **Bibliography & References**

442

443 Arimoto, K., Fukuda, H., Imajoh-Ohmi, S., Saito, H., and Takekawa, M. (2008). Formation of
444 stress granules inhibits apoptosis by suppressing stress-responsive MAPK pathways. Nat Cell
445 Biol *10*, 1324-1332.
446 Belott, C., Janis, B., and Menze, M.A. (2020). Liquid-liquid phase separation promotes animal
447 desiccation tolerance. Proc Natl Acad Sci U S A *117*, 27676-27684.
448 Biegert, A., and Soding, J. (2008). De novo identification of highly diverged protein repeats by
449 probabilistic consistency. Bioinformatics *24*, 807-814.
450 Boeynaems, S., Alberti, S., Fawzi, N.L., Mittag, T., Polymenidou, M., Rousseau, F., Schymkowitz,
451 J., Shorter, J., Wolozin, B., Van Den Bosch, L.*, et al.* (2018). Protein Phase Separation: A New
452 Phase in Cell Biology. Trends Cell Biol *28*, 420-435.
453 Boija, A., Klein, I.A., Sabari, B.R., Dall'Agnese, A., Coffey, E.L., Zamudio, A.V., Li, C.H., Shrinivas,
454 K., Manteiga, J.C., Hannett, N.M.*, et al.* (2018). Transcription Factors Activate Genes through
455 the Phase-Separation Capacity of Their Activation Domains. Cell *175*, 1842-1855 e1816.
456 Boothby, T.C., Tapia, H., Brozena, A.H., Piszkiewicz, S., Smith, A.E., Giovannini, I., Rebecchi, L.,
457 Pielak, G.J., Koshland, D., and Goldstein, B. (2017). Tardigrades Use Intrinsically Disordered
458 Proteins to Survive Desiccation. Mol Cell *65*, 975-984 e975.
459 Bortner, C.D., and Cidlowski, J.A. (2002). Cellular mechanisms for the repression of apoptosis.
460 Annu Rev Pharmacol Toxicol *42*, 259-281.
461 Bracha, D., Walls, M.T., and Brangwynne, C.P. (2019). Probing and engineering liquid-phase
462 organelles. Nat Biotechnol *37*, 1435-1445.
463 Bracha, D., Walls, M.T., Wei, M.T., Zhu, L., Kurian, M., Avalos, J.L., Toettcher, J.E., and
464 Brangwynne, C.P. (2018). Mapping Local and Global Liquid Phase Behavior in Living Cells Using
465 Photo-Oligomerizable Seeds. Cell *175*, 1467-1480 e1413.
466 Brunette, T.J., Parmeggiani, F., Huang, P.S., Bhabha, G., Ekiert, D.C., Tsutakawa, S.E., Hura, G.L.,
467 Tainer, J.A., and Baker, D. (2015). Exploring the repeat protein universe through computational
468 protein design. Nature *528*, 580-584.
469 Bussell, R., Jr., and Eliezer, D. (2003). A structural and functional role for 11-mer repeats in
470 alpha-synuclein and other exchangeable lipid binding proteins. J Mol Biol *329*, 763-778.

471 Chakrabortee, S., Meersman, F., Kaminski Schierle, G.S., Bertoncini, C.W., McGee, B., Kaminski,
472 C.F., and Tunnacliffe, A. (2010). Catalytic and chaperone-like functions in an intrinsically
473 disordered protein associated with desiccation tolerance. Proc Natl Acad Sci U S A *107*, 16084-
474 16089.
475 Choi, J.M., Holehouse, A.S., and Pappu, R.V. (2020). Physical Principles Underlying the Complex
476 Biology of Intracellular Phase Transitions. Annu Rev Biophys *49*, 107-133.
477 Dijksterhuis, J., Nijsse, J., Hoekstra, F.A., and Golovina, E.A. (2007). High viscosity and anisotropy
478 characterize the cytoplasm of fungal dormant stress-resistant spores. Eukaryot Cell *6*, 157-170.
479 Erdos, G., and Dosztanyi, Z. (2020). Analyzing Protein Disorder with IUPred2A. Curr Protoc
480 Bioinformatics *70*, e99.
481 Furuki, T., Niwa, T., Taguchi, H., Hatanaka, R., Kikawada, T., and Sakurai, M. (2019). A LEA model
482 peptide protects the function of a red fluorescent protein in the dry state. Biochem Biophys Rep
483 *17*, 27-31.
484 Geng, X., Guo, J., Zang, X., Chang, C., Shang, H., Wei, H., and Xu, C. (2019). Proteomic analysis of
485 eleven tissues in the Chinese giant salamander (Andrias davidianus). Sci Rep *9*, 16415.
486 Gimenez-Andres, M., Copic, A., and Antonny, B. (2018). The Many Faces of Amphipathic
487 Helices. Biomolecules *8*.
488 Gupta, I., Singh, K., Varshney, N.K., and Khan, S. (2018). Delineating Crosstalk Mechanisms of
489 the Ubiquitin Proteasome System That Regulate Apoptosis. Front Cell Dev Biol *6*, 11.
490 Hand, S.C., Menze, M.A., Toner, M., Boswell, L., and Moore, D. (2011). LEA proteins during
491 water stress: not just for plants anymore. Annu Rev Physiol *73*, 115-134.
492 Hayashi, H., Campenot, R.B., Vance, D.E., and Vance, J.E. (2009). Protection of neurons from
493 apoptosis by apolipoprotein E-containing lipoproteins does not require lipoprotein uptake and
494 involves activation of phospholipase Cgamma1 and inhibition of calcineurin. J Biol Chem *284*,
495 29605-29613.
496 Hengherr, S., Brümmer, F., and Schill, R.O. (2008). Anhydrobiosis in tardigrades and its effects
497 on longevity traits. Journal of Zoology *275*, 216-220.
498 Hubstenberger, A., Courel, M., Benard, M., Souquere, S., Ernoult-Lange, M., Chouaib, R., Yi, Z.,
499 Morlot, J.B., Munier, A., Fradet, M.*, et al.* (2017). P-Body Purification Reveals the Condensation
500 of Repressed mRNA Regulons. Mol Cell *68*, 144-157 e145.
501 Hyman, A.A., Weber, C.A., and Julicher, F. (2014). Liquid-liquid phase separation in biology.
502 Annu Rev Cell Dev Biol *30*, 39-58.
503 Jiang, S., Fagman, J.B., Chen, C., Alberti, S., and Liu, B. (2020). Protein phase separation and its
504 role in tumorigenesis. Elife *9*.
505 Jonsson, K.I., Rabbow, E., Schill, R.O., Harms-Ringdahl, M., and Rettberg, P. (2008). Tardigrades
506 survive exposure to space in low Earth orbit. Curr Biol *18*, R729-R731.
507 Lalli, G., Schott, J.M., Hardy, J., and De Strooper, B. (2021). Aducanumab: a new phase in
508 therapeutic development for Alzheimer's disease? EMBO Mol Med *13*, e14781.
509 Li, F., Jiang, T., Li, Q., and Ling, X. (2017). Camptothecin (CPT) and its derivatives are known to
510 target topoisomerase I (Top1) as their mechanism of action: did we miss something in CPT
511 analogue molecular targets for treating human disease such as cancer? Am J Cancer Res *7*,
512 2350-2394.

513 Li, S., Chakraborty, N., Borcar, A., Menze, M.A., Toner, M., and Hand, S.C. (2012). Late
514 embryogenesis abundant proteins protect human hepatoma cells during acute desiccation.
515 Proc Natl Acad Sci U S A *109*, 20859-20864.
516 Li, W., and Lee, M.K. (2005). Antiapoptotic property of human alpha-synuclein in neuronal cell
517 lines is associated with the inhibition of caspase-3 but not caspase-9 activity. J Neurochem *93*,
518 1542-1550.
519 Makarova, K.S., Aravind, L., Wolf, Y.I., Tatusov, R.L., Minton, K.W., Koonin, E.V., and Daly, M.J.
520 (2001). Genome of the extremely radiation-resistant bacterium Deinococcus radiodurans
521 viewed from the perspective of comparative genomics. Microbiol Mol Biol Rev *65*, 44-79.
522 Mertens, J., Aliyu, H., and Cowan, D.A. (2018). LEA Proteins and the Evolution of the WHy
523 Domain. Appl Environ Microbiol *84*.
524 Neuman, Y. (2006). Cryptobiosis: a new theoretical perspective. Prog Biophys Mol Biol *92*, 258-
525 267.
526 Obexer, P., and Ausserlechner, M.J. (2014). X-linked inhibitor of apoptosis protein - a critical
527 death resistance regulator and therapeutic target for personalized cancer therapy. Front Oncol
528 *4*, 197.
529 Parry, B.R., Surovtsev, I.V., Cabeen, M.T., O'Hern, C.S., Dufresne, E.R., and Jacobs-Wagner, C.
530 (2014). The bacterial cytoplasm has glass-like properties and is fluidized by metabolic activity.
531 Cell *156*, 183-194.
532 Rao, P.N., Reddy, K.S., and Bhuyan, A.K. (2009). Amyloid fibrillation of human Apaf-1 CARD.
533 Biochemistry *48*, 7656-7664.
534 Rasheed, S., Nelson-Rees, W.A., Toth, E.M., Arnstein, P., and Gardner, M.B. (1974).
535 Characterization of a newly derived human sarcoma cell line (HT-1080). Cancer *33*, 1027-1033.
536 Schellenberg, G.D., D'Souza, I., and Poorkaj, P. (2000). The genetics of Alzheimer's disease. Curr
537 Psychiatry Rep *2*, 158-164.
538 Segrest, J.P., Jones, M.K., De Loof, H., Brouillette, C.G., Venkatachalapathi, Y.V., and
539 Anantharamaiah, G.M. (1992). The amphipathic helix in the exchangeable apolipoproteins: a
540 review of secondary structure and function. J Lipid Res *33*, 141-166.
541 Shin, Y., and Brangwynne, C.P. (2017). Liquid phase condensation in cell physiology and disease.
542 Science *357*.
543 Stanton, B.Z., Chory, E.J., and Crabtree, G.R. (2018). Chemically induced proximity in biology
544 and medicine. Science *359*.
545 Tanaka, S., Tanaka, J., Miwa, Y., Horikawa, D.D., Katayama, T., Arakawa, K., Toyoda, A., Kubo, T.,
546 and Kunieda, T. (2015). Novel mitochondria-targeted heat-soluble proteins identified in the
547 anhydrobiotic Tardigrade improve osmotic tolerance of human cells. PLoS One *10*, e0118272.
548 Theillet, F.X., Binolfi, A., Frembgen-Kesner, T., Hingorani, K., Sarkar, M., Kyne, C., Li, C., Crowley,
549 P.B., Gierasch, L., Pielak, G.J.*, et al.* (2014). Physicochemical properties of cells and their effects
550 on intrinsically disordered proteins (IDPs). Chem Rev *114*, 6661-6714.
551 Tolleter, D., Jaquinod, M., Mangavel, C., Passirani, C., Saulnier, P., Manon, S., Teyssier, E., Payet,
552 N., Avelange-Macherel, M.H., and Macherel, D. (2007). Structure and function of a
553 mitochondrial late embryogenesis abundant protein are revealed by desiccation. Plant Cell *19*,
554 1580-1589.
555 Wall, M.E., Wani, M.C., Cook, C.E., Palmer, K.H., McPhail, A.T., and Sim, G.A. (1966). Plant
556 Antitumor Agents. I. The Isolation and Structure of Camptothecin, a Novel Alkaloidal Leukemia

557 and Tumor Inhibitor from Camptotheca acuminata1,2. Journal of the American Chemical
558 Society *88*, 3888-3890.
559 Yagi-Utsumi, M., Aoki, K., Watanabe, H., Song, C., Nishimura, S., Satoh, T., Yanaka, S., Ganser,
560 C., Tanaka, S., Schnapka, V.*, et al.* (2021). Desiccation-induced fibrous condensation of CAHS
561 protein from an anhydrobiotic tardigrade. bioRxiv, 2021.2006.2022.449423.
562 Yamazaki, Y., Zhao, N., Caulfield, T.R., Liu, C.C., and Bu, G. (2019). Apolipoprotein E and
563 Alzheimer disease: pathobiology and targeting strategies. Nat Rev Neurol *15*, 501-518.
564 Yasuda, S., Tsuchiya, H., Kaiho, A., Guo, Q., Ikeuchi, K., Endo, A., Arai, N., Ohtake, F., Murata, S.,
565 Inada, T.*, et al.* (2020). Stress- and ubiquitylation-dependent phase separation of the
566 proteasome. Nature *578*, 296-300.
567

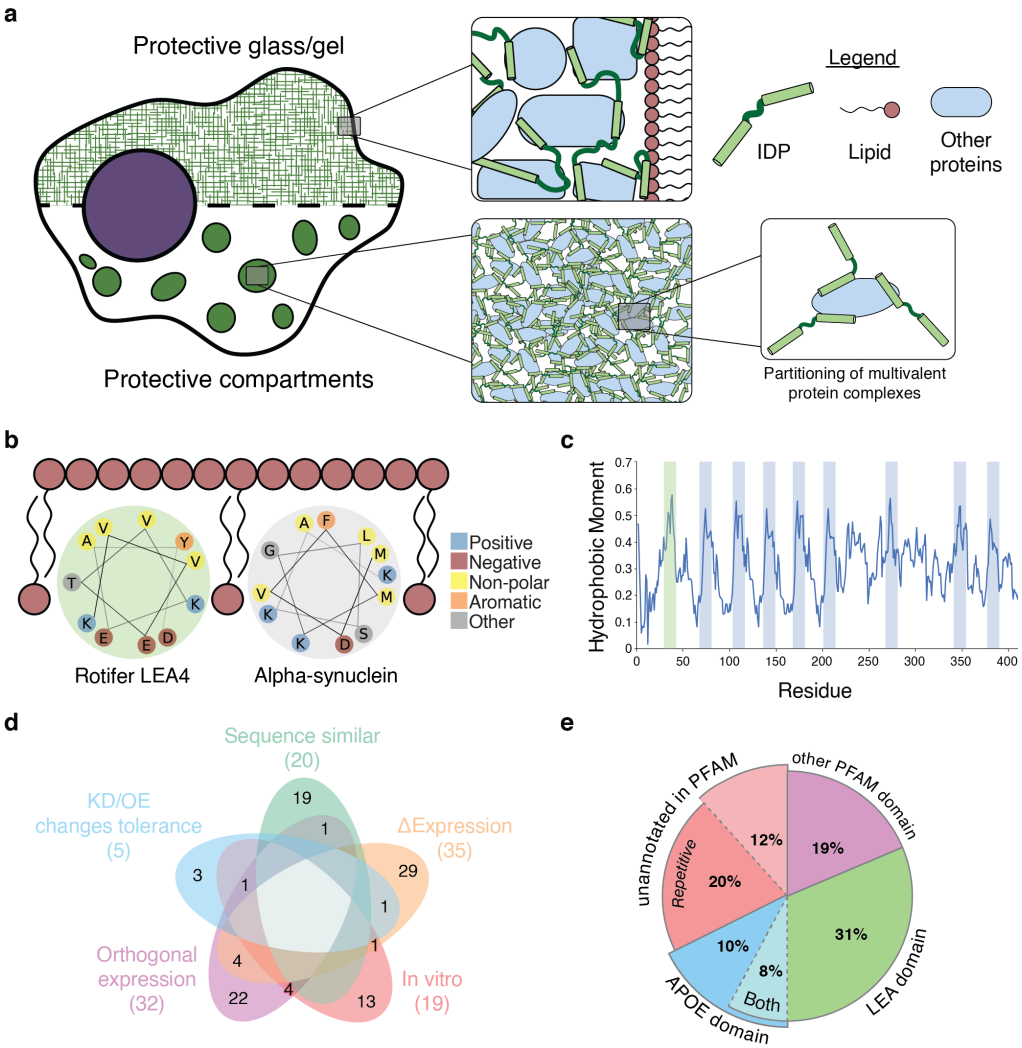

Figure 1: Selection of candidate extremotolerance-associated proteins (a) Illustration of different protective models for cellular stress tolerance. **(b)** Illustration of amphipathic membrane interaction for rotifer LEA4 protein and Alpha-synuclein, thus highlighting a feature indicative of extremotolerance-associated proteins. **(c)** Hydrophobic moment analysis of rotifer LEA4, showing the repetitive nature of the amphipathic signature. Highlighted green segment corresponds to the LEA4 helix in (b). **(d)** Venn diagram of the lines of evidence used to select targets in the final library. Abbreviations: KD, knockdown; OE, overexpression; Δ, change in expression levels. **(e)** Domain analysis of included targets reveals LEA and ApoE domains in almost half of the targets tested. The other half contains proteins with other PFAM domains (19%) or without any affiliated PFAM entry (32%). Of the proteins lacking a known PFAM annotation, many exhibit repetitive sequence (20% of all targets).

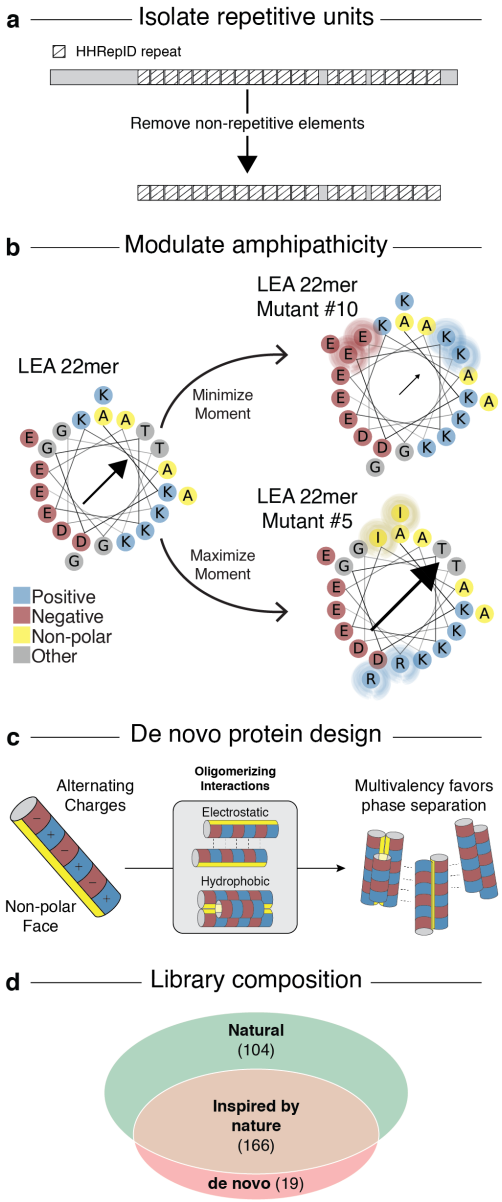

Figure 2: Design based on candidate extremotolerance-associated proteins (a) Truncations were made to isolate regions of repetitive and amphipathic sequence. **(b)** Small helices were selected and altered based on their hydrophobic moment. **(c)** Synthetic alpha helix-containing proteins designed to oligomerize. **(d)** Venn diagram highlighting the library that was tested.

23

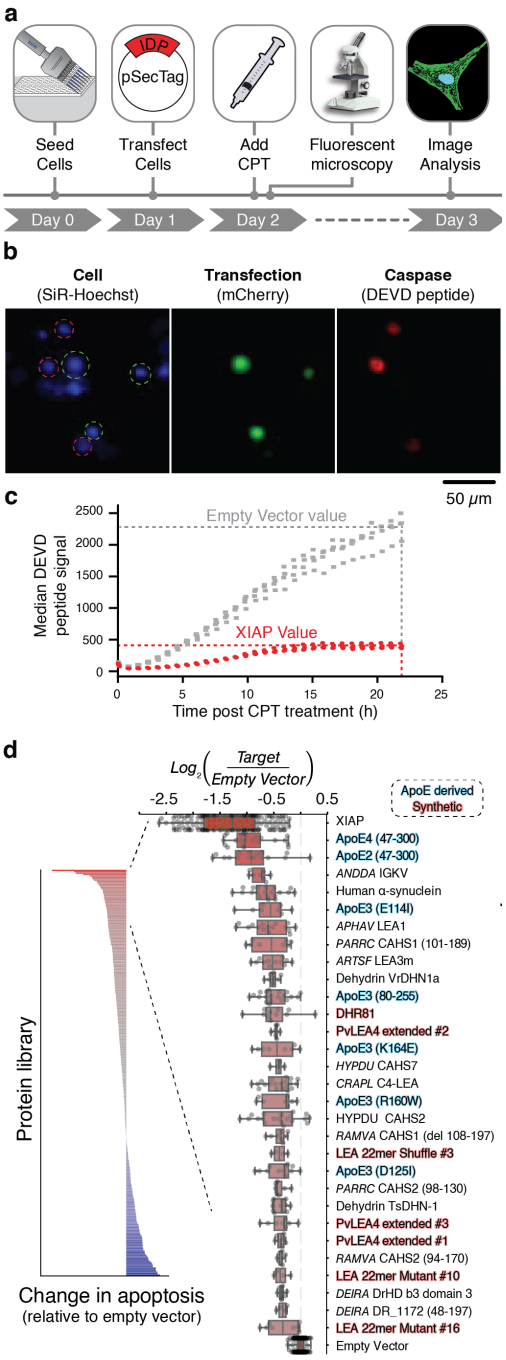

25 **Figure 3: Screen for CPT resistance by extremotolerance-associated proteins (a)**
26 Flow diagram of the assay. **(b)** Representative images showing cells during the assay.
27 Cells are identified using SiR-Hoechst marking the nucleus (*blue*). Transfected cells are
28 identified by the presence of the mCherry marker (*green*). Finally, the degree of apoptosis
29 is identified by the presence of the cleaved DEVD peptide (*red*). **(c)** Positive control
30 showing apoptosis reduction upon expression of XIAP. **(d)** Bar graph highlighting the

apoptosis resistance provided by different constructs, including zoomed in area to highlight the top hits in the assay. Source species of a sequence are abbreviated and shown in italics; abbreviations are drawn from Uniprot, including *RAMVA* (*Ramazzottius varieornatus*), *HYPDU* (*Hypsibius dujardini*), *PARRC* (Paramacrobiotus richtersi), *ANDDA* (*Andrias davidianus*), *APHAV* (*Aphelenchus avenae*), *ARTSF* (*Artemia franciscana*), *CRAPL* (*Craterostigma plantagineum*), and *DEIRA* (*Deinococcus radiodurans*).

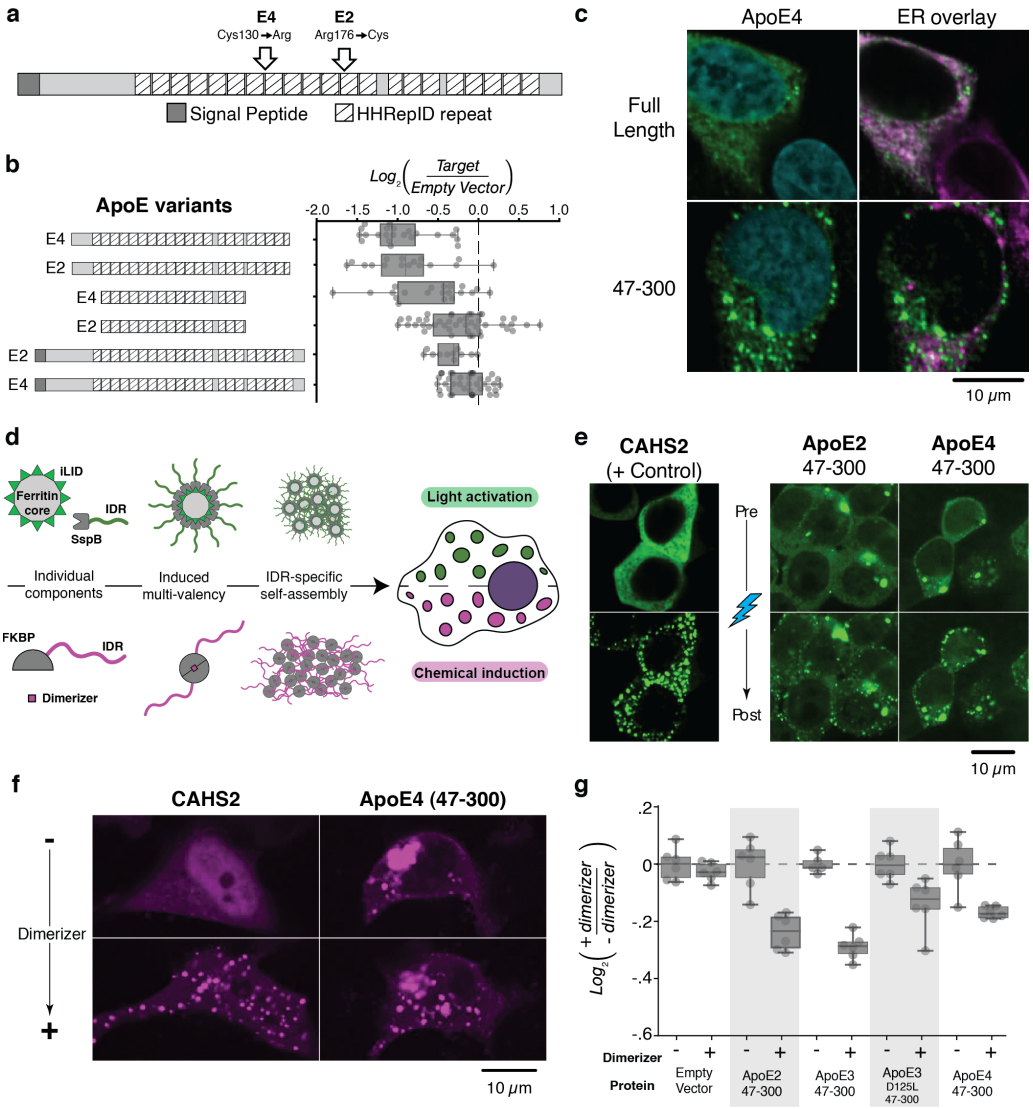

Fig. 4. ApoE truncations and synthetic condensates further reduce apoptosis. **(a)** Gene diagram highlighting the repetitive region of ApoE. **(b)** Boxplots highlighting the apoptosis assay performance of the full length and truncated forms of ApoE2 and E4. **(c)** Immunofluorescence of ApoE4, full length and truncated forms. *White* indicates colocalization, which is more apparent with the full-length protein. The truncated form appears to exhibit larger and more distinguishable puncta. **(d)** Diagram of the induced multi-valency systems used here, including the light-inducible system (*top*) and the chemically-inducible system (*bottom*). **(e)** Condensate formation assay using the light-inducible system, including the CAHS2 positive control showing condensates only upon light induction and several ApoE examples that form condensates both before and after induction. **(f)** Condensate formation assay using the chemically-inducible system, including the CAHS2 positive control showing condensates only upon added dimerizer and ApoE4 (47-300) exhibiting condensates both before and after induction. **(g)**

Apoptosis data showing reduction in apoptosis upon condensate induction with dimerizer. Data are normalized to mean apoptosis level of uninduced (i.e. no dimerizer) sample for each construct.

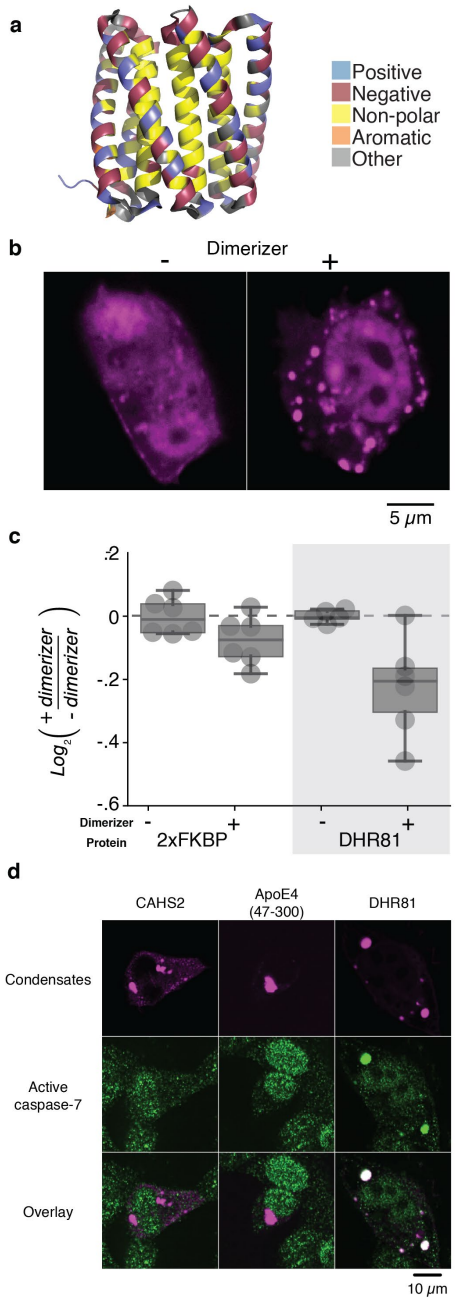

Fig. 5. DHR81 condensate formation and apoptosis reduction. (a) Diagram of DHR81, illustrating a charge distribution that can support oligomerization. **(b)** Sample images highlighting how the synthetic protein DHR81 supports chemically-induced condensates. **(c)** Apoptosis is further reduced in the presence of dimerizer (i.e. with induced DHR81 condensates). The FKBP-modifications alone, which enable chemically-induced multi-valency, have a minimal effect on apoptosis. **(d)** Activated caspase-7 (*green*) co-localizes with DHR81 condensates but not CAHS2 or ApoE4 (47-300) condensates (*magenta*). *White* indicates colocalization.

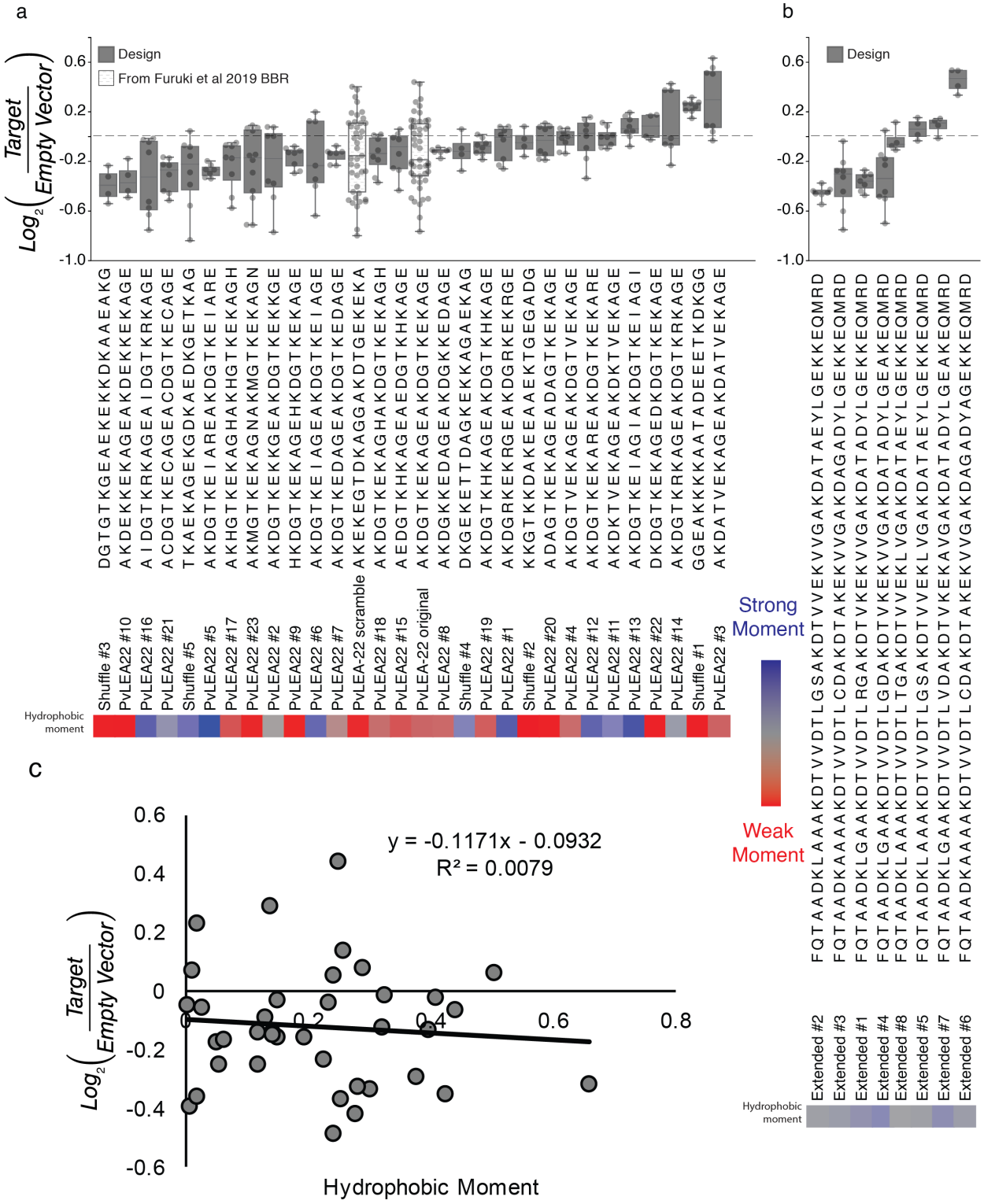

Figure 3 Supplement (a) Graph and sequences of various LEA repeats tested, with full sequences and performance. **(b)** Graph and sequences of extended LEA repeats tested.

(c) Correlation analysis for relationship between hydrophobic moment with apoptosis assay performance.

73

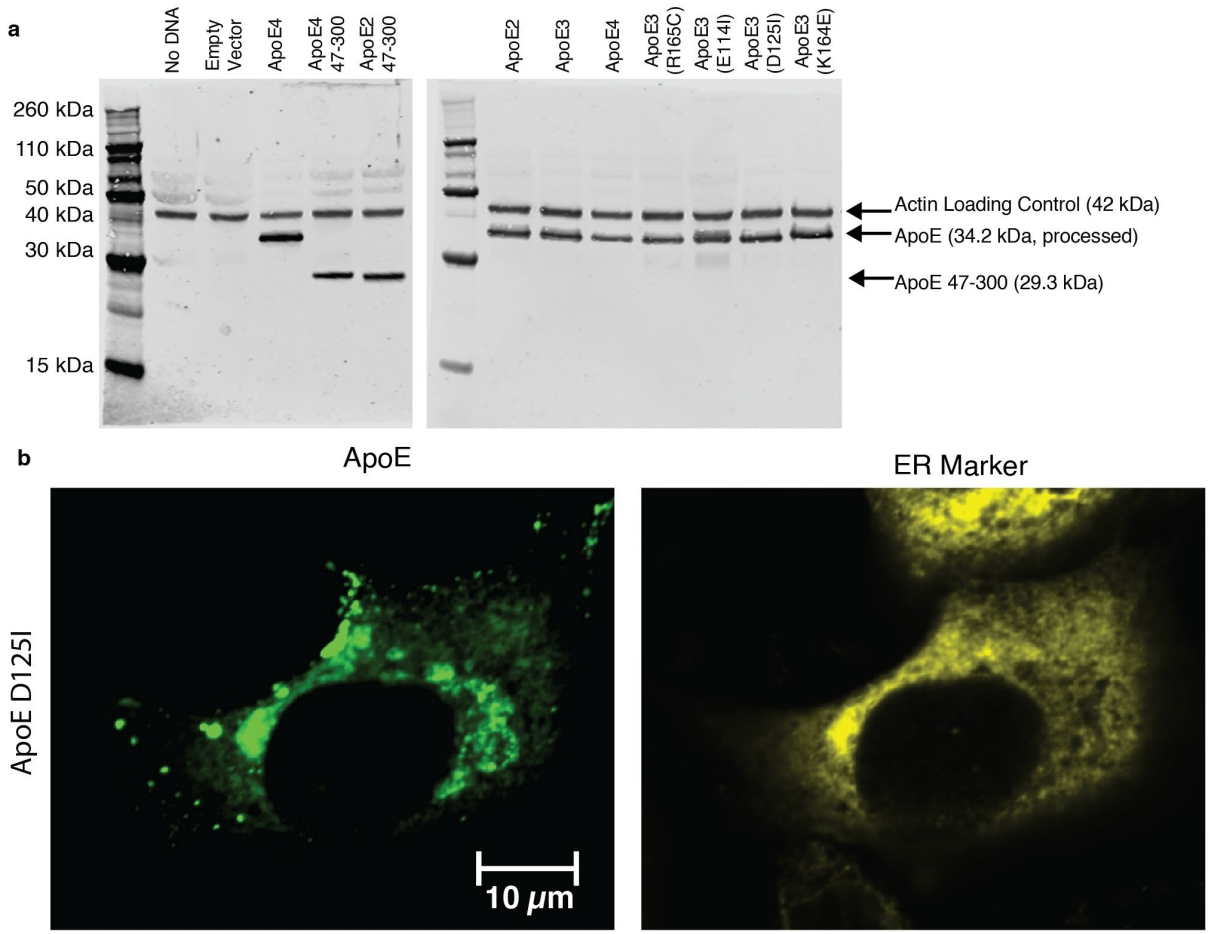

75 **Figure 4 Supplement (a)** Western blot data of some ApoE constructs showing
76 expression at the expected molecular weight **(b)** Sample images showing condensates
77 forming in the full length ApoE3 D125I mutation.

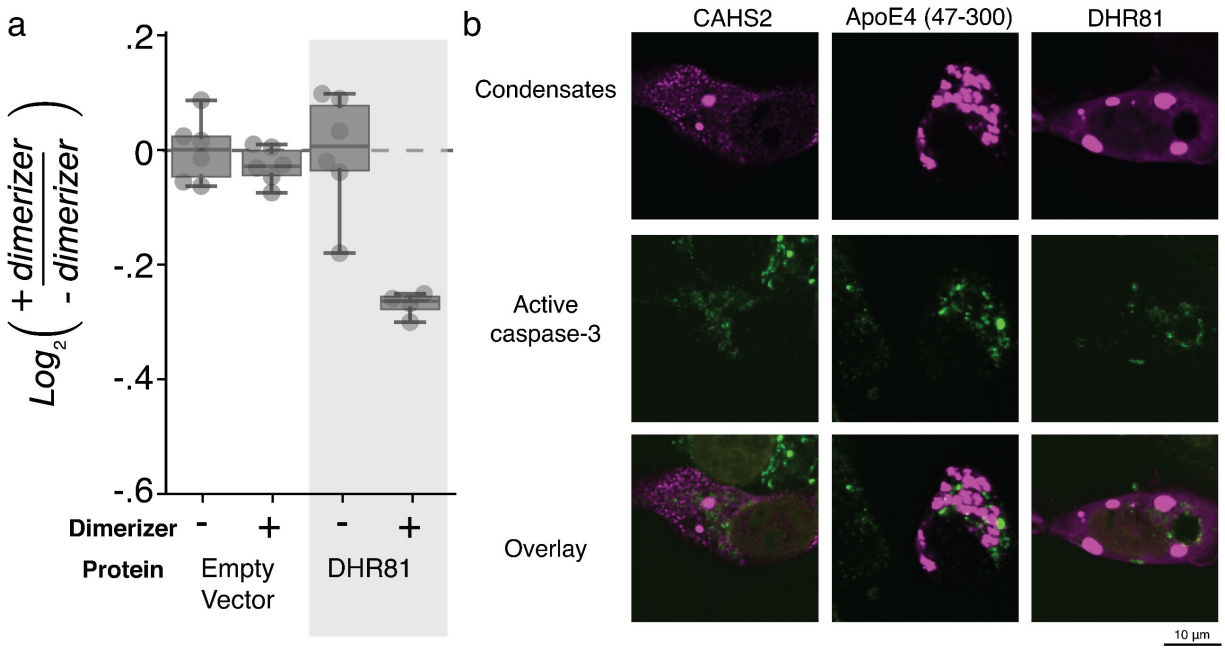

79 **Figure 5 Supplement** (a) DHR81 inducible condensates reduce apoptosis. (b) Sample
80 images showing no co-localization between activated caspase 3 and condensates.